1-1-1995

# A theoretical study of surface kinetic processes in the Mbe growth of compound semiconductors

Shridhar Gangadhar Bendi
*University of Nevada, Las Vegas*

## Repository Citation

Bendi, Shridhar Gangadhar, "A theoretical study of surface kinetic processes in the Mbe growth of compound semiconductors" (1995). *UNLV Retrospective Theses & Dissertations*. 511.
http://dx.doi.org/10.25669/4v8m-005q

## INFORMATION TO USERS

This manuscript has been reproduced from the microfilm master. UMI films the text directly from the original or copy submitted. Thus, some thesis and dissertation copies are in typewriter face, while others may be from any type of computer printer.

**The quality of this reproduction is dependent upon the quality of the copy submitted.** Broken or indistinct print, colored or poor quality illustrations and photographs, print bleedthrough, substandard margins, and improper alignment can adversely affect reproduction.

In the unlikely event that the author did not send UMI a complete manuscript and there are missing pages, these will be noted. Also, if unauthorized copyright material had to be removed, a note will indicate the deletion.

Oversize materials (e.g., maps, drawings, charts) are reproduced by sectioning the original, beginning at the upper left-hand corner and continuing from left to right in equal sections with small overlaps. Each original is also photographed in one exposure and is included in reduced form at the back of the book.

Photographs included in the original manuscript have been reproduced xerographically in this copy. Higher quality 6" x 9" black and white photographic prints are available for any photographs or illustrations appearing in this copy for an additional charge. Contact UMI directly to order.

UMI

A Bell & Howell Information Company
300 North Zeeb Road, Ann Arbor, MI 48106-1346 USA
313/761-4700 800/521-0600

# A THEORETICAL STUDY OF SURFACE KINETIC PROCESSES IN THE MBE GROWTH OF COMPOUND SEMICONDUCTORS

by

Shridhar G. Bendi

A thesis submitted in partial fulfillment
of the requirements for the degree of

Master of Science

in

Electrical and Computer Engineering

Department of Electrical and Computer Engineering
University of Nevada, Las Vegas
August, 1995

The thesis of Shridhar G. Bendi for the degree of Master of Science
in Electrical and Computer Engineering is approved.

R.

Chairperson, Ramasubramanian Venkatasubramanian, Ph.D

William L. Brogan

Examining Committee Member, William L. Brogan, Ph.D

Ashok Iyer.

Examining Committee Member, Ashok Iyer, Ph.D

Ajoy Kumar Datta

Graduate Faculty Representative, Ajoy K. Datta, Ph.D

Cheryl L Bowles

Interim Dean of Graduate College, Cheryl Bowles, Ed.D

University of Nevada, Las Vegas
August, 1995

# ABSTRACT

The surface kinetics processes in the molecular beam epitaxy (MBE) growth of $GaAs$ (100) and the MBE doping kinetics are studied theoretically, using a stochastic model which is based on the master equation approach and random distribution approximation. The kinetic processes included in the model are: adsorption, surface migration and evaporation. In the study of surface roughening kinetics in $GaAs$ (100) diatomic arsenic molecular specie ($As_2$) was used. The time averaged reflection-high-energy-electron -diffraction (RHEED) intensity obtained from the growth data was in agreement with the theoretical results. A transition temperature at which time averaged RHEED intensity is a maximum was observed. The RHEED intensity increases with temperature till the transition temperature due to surface smoothening resulting from the surface migration of $Ga$ and $As$ to energetically favorable sites. The RHEED intensity decreases beyond the transition temperature due to the evaporation of $As$ from the surface. The transition temperature can be explained by the difference in time for the formation of energetically stable surface adatom clusters resulting from the difference in the effective surface migration rates for various flux ratios. The doping studies were performed for various growth conditions. The predicted sticking coefficient of $In$ versus $\frac{1}{T}$ shows excellent agreement with experiments reported in literature. The sticking coefficient decreases with $T$ due to surface segregation aided evaporation of $In$ at higher temperature. The predicted dopant depth profile also shows excellent qualitative agreement with experiments. The surface segregation of $In$ occurs due to a strong repulsive interaction between $In$ and the host lattice. The results of this study show that there is a dopant depleted zone (DDZ) where the $In$ concentration is lower than both the bulk and the top surface layer. The observed DDZ qualitatively matches that observed in experiments. The time and growth rate dependences of the phenomenon are studied and found to be in good agreement with experiments. The model was used to study $\delta$ doping of dopants as a function of temperature. The results are in qualitative agreement with experimental results. With an increase in temperature, the dopant profiles become sharper. This is caused by a smoother growing surface at higher temperatures. Even though, the results of the work qualitatively agree with the experimental work, there is a quantitative difference between the results in terms of dopant profiles. This discrepancy is attributed to the limitation of the model, and the model parameters.

# ACKNOWLEDGEMENTS

I am grateful to my advisor Dr. Venkatasubramanian for his invaluable guidance and support during the course of this effort. His patience and cooperation is integral in making this work possible. I wish to express my thanks to Dr. Ashok Iyer, Dr. William L. Brogan, and Dr. Ajoy K. Datta for serving on my thesis committee.

The constant encouragement, support and love given to me by my parents over the years is indescribable and I am indebted to them forever. I also wish to acknowledge the encouragement and help given by my sister and friends.

# Contents

Abstract . . . . . . . . . . . . . . . . . . . . . . . . . . . . . . . . . . . . . iii
Acknowledgments . . . . . . . . . . . . . . . . . . . . . . . . . . . . . . . . . v

1 INTRODUCTION 1

2 LITERATURE OVERVIEW 3
2.1 Molecular beam epitaxy . . . . . . . . . . . . . . . . . . . . . . . . . . . . 3
2.2 *GaAs* Experimental Studies . . . . . . . . . . . . . . . . . . . . . . . . . 5
2.2.1 Review of Experimental Studies . . . . . . . . . . . . . . . . . . . 5
2.3 Doping . . . . . . . . . . . . . . . . . . . . . . . . . . . . . . . . . . . . 7
2.4 Theoretical Analysis . . . . . . . . . . . . . . . . . . . . . . . . . . . . . 9

3 Surface Kinetic Processes in the MBE Growth of GaAs (100) 15
3.1 The Stochastic Model . . . . . . . . . . . . . . . . . . . . . . . . . . . . 15
3.1.1 Macrovariables . . . . . . . . . . . . . . . . . . . . . . . . . . . . 17
3.1.2 Boundary Conditions . . . . . . . . . . . . . . . . . . . . . . . . . 19
3.2 The *GaAs* system : the model and output parameters . . . . . . . . . . . 20
3.3 Results and discussions . . . . . . . . . . . . . . . . . . . . . . . . . . . 22
3.4 Summary . . . . . . . . . . . . . . . . . . . . . . . . . . . . . . . . . . . 25

4 MBE Doping Kinetics 31
4.1 Rate Equation Model for Doping . . . . . . . . . . . . . . . . . . . . . . . 31
4.2 Results and Discussion . . . . . . . . . . . . . . . . . . . . . . . . . . . . 34
4.2.1 In doping of Si . . . . . . . . . . . . . . . . . . . . . . . . . . . . 34
4.2.2 Delta Doping of Si . . . . . . . . . . . . . . . . . . . . . . . . . . 38
4.3 Summary . . . . . . . . . . . . . . . . . . . . . . . . . . . . . . . . . . . 40

5 Conclusion 48
BIBLIOGRAPHY . . . . . . . . . . . . . . . . . . . . . . . . . . . . . . . . 50

# List of Figures

3.1 A schematic representation of atomistic picture of all the kinetic processes that are considered for the simulation: (1) incorporation, (2) surface migration, (3) reevaporation. . . . . . . . . . . . . . . . . . . . . . . . . . . . 26
3.2 A pictorial representation of the MSOS restrictions. . . . . . . . . . . . . . 27
3.3 Concentration profiles of $Ga$ and $As$ for flux ratio 1:10 for various temperatures. (a) 823K (b) 848K (c) 873K. . . . . . . . . . . . . . . . . . . . . . . 28
3.4 Concentration profiles of $Ga$ and $As$ for flux ratio 1:20 for various temperatures. (a) 823K (b) 848K (c) 873K. . . . . . . . . . . . . . . . . . . . . . . 29
3.5 Time averaged RHEED intensity versus temperature for flux ratios (a) 1:10 (b) 1:20. . . . . . . . . . . . . . . . . . . . . . . . . . . . . . . . . . . . . 30

4.1 Sticking coefficient of the dopant, $In$, versus $\frac{1}{T}$. . . . . . . . . . . . . . . . . 42
4.2 Dopant segregation profile for various growth times for growth at 933°K. . 43
4.3 Dopant segregation profiles for various temperatures for a growth time of 20 seconds. . . . . . . . . . . . . . . . . . . . . . . . . . . . . . . . . . . . . . . 44
4.4 Dopant sticking coefficient for various growth rates at 933°K. . . . . . . . . 45
4.5 Surface concentration of dopant for various growth times at 933°K. . . . . 46
4.6 Delta doping profiles with (a) $E_{SID}$ = -0.08 eV (strong repulsion) and (b) $E_{SID}$ = -0.01 eV (weak repulsion) at 933°K. . . . . . . . . . . . . . . . . . . 47

# Chapter 1

# INTRODUCTION

With the advent of ultra-high vacuum technique of molecular beam epitaxy (MBE), heterostructures consisting of dissimilar materials have been successfully grown and exploited to fabricate novel microstructures such as superlattices and quantum well structures, and therfore has opened up new areas in both device technology and semiconductor physics. The performance of devices fabricated critically depends on the interfacial roughness in heterostructures and the quality of doped and undoped epilayers grown. To achieve device quality, it is of great importance to understand the growth kinetics of material used for growing crystal and also to study the dopant segregation phenomenon.

MBE growth and doping kinetics of many elemental and compound semiconductors has been studied experimentally [3-6,18-22,28-32] and theoretically [9-17,23,27] in the past decade. Of these materials, $GaAs$ and $Si$ have had considerable attention due to their technological advantages over the other materials. Despite numerous studies, there is a considerable lack of understanding of growth kinetics and its relation to the growth parameters. The subject of this thesis is to theoretically address two growth issues: surface roughening kinetics of $GaAs$ (100) and $Si$ doping kinetics.

Traditionally the theoretical tools employed for MBE kinetic studies are Monte Carlo (MC) simulations [11,12], Molecular Dynamics (MD), and Stochastic Models [7,13-15]. MC simulation is crystal size limited, but provides microstructural details of thin film surfaces and interfaces. MD simulation provides atomistic details and is very rigorous, but is computationally intensive due to pico second time scale of simulation. The stochastic model approach is not size limited, but does not provide microstructural details of the thin film. Since for the problems to be addressed, crystal size limitation should be avoided and macroscopic roughness ($GaAs$) and spatial distribution of dopant ($Si$) can be obtained without need for microstructural details, the stochastic model approach is adopted for this thesis.

## Overview of the Thesis

This thesis theoretically addresses the issues of surface roughening kinetics in the MBE growth of (100) $GaAs$ and surface segregation phenomenon during $In$ doping of $Si$ using the stochastic model and the rate equation model, respectively. A brief literature survey, discussing both experimental and theoretical models for surface kinetic processes in the MBE growth of $GaAs$ (100) and MBE doping kinetics of $Si$ is presented in Chapter 2. The detailed study of surface roughening kinetics in $GaAs$ (100) using stochastic model of MBE growth is presented in Chapter 3. Chapter 4 includes the detailed study of MBE doping kinetics in $In$ doped $Si$ system and $\delta$ doping kinetics using the rate equation model which is a simplified stochastic model. The conclusions are stated in Chapter 5.

# Chapter 2

# LITERATURE OVERVIEW

Molecular Beam Epitaxy (MBE) is one of the most suited techniques for growing high crystalline quality epilayers with great purity and precise thickness control of semiconductor compounds. In this section, the experimental work on $GaAs$ MBE growth and in situ doping in MBE growth of semiconductors are reviewed along with the theoretical work.

## 2.1 Molecular beam epitaxy

The technology of crystal growth has advanced enormously during the past two decades. Among the many advances, the development and refinement of molecular beam epitaxy (MBE) has been the most important one. Crystals grown by MBE are precisely controlled and they form the basis for the most advanced microstructures such as superlattices and quantum well structures of which high speed and high frequency opto-electronic devices are fabricated.

MBE is an epitaxial process involving the reaction of one or more thermal beams of atoms or molecules with crystalline surface under ultra high vacuum ($10^{-9}$ torrs) conditions. MBE can achieve precise control in both chemical compositions and doping profiles. In this growth method, the incorporation of impinging atoms (film constituent or dopant) into the film during growth is controlled by the surface adsorption-desorption-migration kinetics (the so called sticking process) rather than by near-equilibrium thermodynamics, as is the case with other conventional growth techniques such as Chemical Vapor Deposition (CVD) or Liquid Phase Epitaxy (LPE).

MBE crystal growth occurs via the reaction and condensation of molecules that arrive at the surface, rather than viscous or diffusive, flow. In other words, molecules do not collide with one another enroute to the substrate, and the molecules that miss or leave the substrate are pumped away almost instantaneously. As a result, multilayered structures with extremely abrupt interfaces can be grown and microscopic processes occuring on the surface apart from the diffusion-controlled mass and/or heat transport to and from the surface can be studied.

The most important aspect of MBE is the facility to control the growth processes at the atomic or molecular scales (a few $\AA$). With the conventional crystal growth techniques, growth processes can be controlled only in the macroscopic scale (a few $100\AA$). MBE, in contrast to the conventional growth techniques, allows to kinetically control the microscopic surface kinetic processes of the growth of thin films due to the following features:

- Low growth temperatures employed in MBE growth minimize the bulk diffusion of atoms in the growing crystals resulting in the surface kinetic processes dominating the growth.

- The ultra high vacuum of the MBE system facilitates well collimated beams and maintains clean crystal surfaces, while the use of nearly perfect single crystals as substrates produces atomistically smooth surfaces.

- In addition, a variety of in-situ analytical tools such as reflection high energy electron diffraction (RHEED), Auger electron spectroscopy (AES) flux monitors, and substrate temperature monitors facilitate continuous monitoring and atomic level control of the growth process.

## 2.2 *GaAs* Experimental Studies

### 2.2.1 Review of Experimental Studies

There has been a series of [1-15] experimental and theoretical attempts to understand the origin of the surface kinetic processes in the MBE growth of $GaAs$ (100). Foxon et. al. [3] studied the kinetics of $Ga$ and $As_4$ interaction on $GaAs$ (100) surfaces. In the temperature range $300-400^oK$ $As_4$ is non-dissociating chemisorbed on $Ga$ atoms from a weakly bound precursor state, but above $450^oK$ there is a pairwise dissociation-recombination reaction between $As_4$ molecules adsorbed on adjacent $Ga$ lattice sites. At temperatures higher than $600^oK$ a temperature dependent $Ga$ adatom population is formed by the desorption of $As_2$ from the surface. Thus above $450^oK$, it is possible to produce $GaAs$ from beams of elements, but below this temperature the stoichiometric compound does not form.

Foxon et. al. [4] used modulated beam technique to study the kinetics of $GaAs$ (100) surfaces. In the temperature range $300-600^oK$ they found surface association reaction to occur, leading to the desorption of $As_4$ by a first order process. Above $600^oK$, $As_2$ is lost from the substrate itself by a dissociation reaction, which gives rise to a temperature dependent $Ga$ adatom population, and this in turn results in a temperature dependent $As_2$

sticking coefficient which can result unity.

In the case of *GaAs* study [6], a transistion temperature was observed above and below which the surface is rougher. This transition temperature was observed to be flux ratio and temperature dependent. The kinetics of surface roughening in this case was explained in terms of competition between the surface roughening processes such as adsorption and evaporation and the surface smoothening process such as the migration of atoms to energetically stable sites.

Foxon et. al. [5] discussed the growth of binary compounds such as *GaAs* and alloys with mixed group III and mixed group V elements. He also discussed the relation between growth conditions and resulting film properties for binary compounds, alloys, and interfaces. The *Ga* and *As* populations present on the surface during growth depend on both substrate temperature and the relative fluxes of *Ga* and *As* atoms reaching the surface. As the substrate temperature is increased, the sticking coefficient of impurities is reduced and at fixed substrate temperatures increasing the *As* to *Ga* ratio or changing from $As_4$ to $As_2$ reduces the arsenic vacancy concentration.

Foxon et. al. [5] also observed that the properties of $AlGaAs-GaAs$ modulation-doped structures depend upon the order in which the layers are grown. For the so called normal structure where *AlGaAs* is grown on top of *GaAs* the enhanced mobilities are much better and less sensitive to substrate temperatures than the equivalent inverted structures where *GaAs* is grown on top of *AlGaAs* [33]. It has been suggested [33] that it is related to the influence of substrate temperature on the morphology of *AlGaAs*.

Chen et. al. [6] reported a systematic examination of the influence of each growth parameter on the surface kinetic processes in *GaAs* MBE growth by employing RHEED intensity dynamics measurements on $GaAs$ (100). The results reveal the existence of a metastable state regime where the surface migration is favored such as to form an optimal growth front.

## 2.3 Doping

Doping an epilayer during its growth by coevaporating the dopant has been the standard practice in MBE of semiconductors. Due to low growth rates ($1\mu m/hr.$) and low growth temperatures (limited or negligible diffusion), abrupt dopant profiles should be achievable in MBE grown epilayers. However, for most semiconductors doped in-situ, either a smearing of the dopant profile and/or surface enrichment of the dopant have been observed experimentally [16-32]. In addition, it has been observed that some dopants incorporate inefficiently in some semiconductors due to excessive evaporation dictated by low binding energy of the dopants to the growing surface.

Many experimental and theoretical models have been proposed to explain the behaviour of the dopant atoms during the growth of the crystal. Iyer et. al. [16] proposed a kinetic model which described the time evolution of the surface concentration of dopants in terms of incorporation and evaporation. Their model was able to explain many experimental observations in the doping of Si [25]. However, it did not explicitly include the surface segregation phenomenon. Wood et. al. [17] employed the same model for $Mg$ doping of $GaAs$ and arbitrarily assumed that the incorporation coefficient of the dopant is linearly dependent on the growth rate in order to explain their experimental observations.

Bean et. al. [18] presented detailed behaviour of the $n$ type dopant $Sb$. Hyperabrupt doping profiles were produced with a resolution superior to that obtained by CVD epitaxy and $Sb$ surface segregation was also detected for temperature below $850^oC$.

Ota et. al. [19] tried to study n-type doping techniques in $Si$ MBE by simultaneous arsenic ion implantation and by antimony evaporation. They grew high quality $Si$ MBE with an arsenic ion ($As^+$) source or an antimony effusion source. For $As^+$ ions at $600eV$, the sticking coefficient was $> 0.75$ at growth temperatures ranging from 750 to $950^oC$, while that evaporated antimony strongly depended on growth temperature.

Earlier, work with n-type of dopants from separate sources has been performed. Becker et. al. [20] grew epitaxial $Si$ films on single-crystal $Si$ (100) substrates from an electron-gun source in UHV doped with gallium and aluminium from separate oven sources. $Ga$ doping profiles in $Si$ MBE films could be controlled accurately for substrate temperature in the range $10^{14} - 5 \times 10^{17} cm^{-3}$ but precise control of the doping has not been achieved for films doped with aluminium.

A segregation model by Rockett et. al. [21] accounted for the accumulation of $Sn$ at the growing film surface and the corresponding $Sn$ depletion near the film-substrate interface during the deposition of $Sn$-doped $GaAs$ by MBE. The calculated $Sn$ profiles were found to provide a good fit to experimental data obtained by secondary ion mass spectrometry.

Streit et. al. [22] performed doping of $Si$ in MBE systems by solid phase epitaxy. The doped $Si$ films were deposited by controlled coevaporation or $Ga(p)$ or $Sb(n)$ and $Si$ at room temperature on an atomically clean $Si$ substrate in UHV. The amorphous films that were crystallized by heating the substrate to $575^oC$, have advantages over normal evaporative doping during MBE:

(1) unity sticking coefficient of dopant (2) no smearing or carry-over of the dopant (3) better mobility (bulk values of $n$ or $p \sim 10^{18} cm^{-3}$) (4 ) higher doping levels ($>8 \times 10^{18} cm^{-3}$

for $Ga$, $8 \times 10^{19} cm^{-3}$ for $Sb$).

Barnett et. al. [21,23] proposed a model including the segregation phenomenon in which they assumed that dopant atoms within several nanometers of the subsurface diffuse to the surface.

Andrieu et. al. [24] proposed a new mechanism of dopants climbing to the surface and developed a rate equation model based on this assumption. Their model was able to explain the surface segregation phenomenon satisfactorily.

Parry et. al. [25] presented the temperature dependence of incorporation process during heavy Boron doping in $Si$ MBE. Boron doped layers were grown by $Si$ MBE to establish incorporation processes at temperatures between 900 and $450^{o}C$ . For temperature exceeding $650^{o}C$ a surface accumulated phase of Boron was formed when doping levels exceeded solid solubility limits. Above $750^{o}C$, the measured equilibrium solubility limit was in the $10^{19} cm^{-3}$ range. Below $650^{o}C$, the processes leading to the formation of the surface phase were kinetically limited, manifested by a sharp increase in boron solubility limit, with completely activated levels above $1 \times 10^{20} cm^{-3}$. At intermediate temperatures the degree of dopant activation was found to be dependent on growth rate.

## 2.4 Theoretical Analysis

Saito and Krumbhaar [7] studied the influence of the relaxation and the surface diffusion processes on the kinetics of crystal growth. The Saito and Krumbhaar (SK) model is based on the master equation approach with quasi chemical approximation (QCA) and the SOS restriction. The SK model is generalized to crystals with any in-plane coordination number and is applicable to one-sublattice crystal only. By comparing the results of the

MC simulations with that of the SK model, it was shown that the QCA scheme gives rise to reliable results on the kinetics of crystal growth for a chemical potential difference, $\Delta\mu$ (between the vapor and the solid), greater than the critical value, $\Delta\mu_c$, for the existence of metastable state with infinite lifetime below even the roughening point. It was also shown that, in general, the surface diffusion enhances the growth rate and reduces the surface roughness.

Arthur et. al. [8] proposed a kinetic model involving changes in surface stoichiometry which gives quantitative agreement with experiment for both desorption rate and surface composition. His model asssumes that $As_2$ is adsorbed in a weakly-bound molecular precursor state from which dissociation into $As$ atoms in $As$ surface sites occurs. Recombination of surface $As$ atoms into the molecular state was found to happen at a rate whose activation energy decreases rapidly with increasing $As$ concentration in the surface.

Weeks et. al. [9,10] investigated epitaxial crystal growth. The authors utilized the SOS model, in which the crystal is described by an array of columns of atoms with the requirement that no vacancy sites may exist within the crystal, i.e., every atom must possess a nearest neighbor immediately below it. This model for defect-free simple cubic [100] crystal growth was the subject of both analytical and computational approaches. Many aspects of crystal growth were simulated, including evaporation, migration, screw dislocations, and the roughening transistions at high temperatures.

Madhukar et. al. [11] presented a model based on Monte Carlo (MC) simulations to study the RHEED oscillation behaviour as a function of arsenic pressure, $P_{As_2}$ for low substrate temperatures. The oscillations decayed faster for growth with high $P_{As_2}$ compared to that with low $P_{As_2}$. The reason for faster damping is that the growth front roughened faster due to shorter migration length of $Ga$. Shorter migration length and roughened growth front result in high $Ga$ vacancy concentration on the $Ga$ sublattice. The RHEED oscillation amplitude for high temperature growth was larger and the oscillations damped at a very slow rate. This suggests that the growth front roughens at a very slow rate indicating that the $Ga$ atoms arriving on the surface migrate very fast to energetically favorable sites before getting trapped by a chemisorbing $As_2$. In other words, the surface migration rate is much faster than the $As_2$ chemisorption rate on the $GaAs$ surface. Results of their simulation compared well with that of experiments for various conditions of pressures and temperatures. It was concluded that high substrate temperature in conjunction with low $As_2$ to $Ga$ pressure results in sharper growth front and low $Ga$ vacancy concentration in $Ga$ sublattice.

Singh et. al. [12] presented a model for the growth of III-V compound semiconductors by MBE which is based on an atomistic MC simulations and a statistical fluctuation theory. Their model concerns itself with the intrinsic growth mechanism only and does not address the role of extrinsic effects such as the impurities. The model allows one to understand the microscopic nature of the growth front and the interface as well as to identify the critical kinetic parameters responsible for their quality. The model includes the growth parameters such as attachment, inter and intra layer migrations. The kinetics of the growth process are given by impinging flux of the cations ($Ga$), the anion overpressure $P_{As_2}$, the surface migration rates of cations after attaching to the growing surface, and the evaporation rates of the atoms. The evaporation is assumed to be little and the incorporation rate to be unity. Singh et. al. studied the the effect of surface migration of $Ga$ on the kinetics-controlled roughening of (100) $GaAs$ by MC simulation. It was observed that the growth mode changed from two dimensional to three dimensional with increasing substrate temperature, resulting in a roughening transistion for (100) $GaAs$. It was pointed that the roughening transistion described by Burton et. al. (1951) (Burton, Cabrera, Frank) (BCF) differs from what they observed. The roughening transistion of BCF is based on the energetics only, and occurs at a specific temperature, whereas the roughening that Singh et. al. (1983) observed, is kinetically controlled and is dependent on the impingement rate and the surface migration kinetics of $Ga$.

Ghaisas et. al. (1985) using the MC technique, identified two different types of Configuration Dependent Reactive Incorporation (CDRI) mechanisms i.e. Reaction Limited Incorporation (RLI) and Configuration Limited Reactive Incorporation (CLRI). In the case of RLI growth, the rates of dissociative chemisorption reactions of $As_2$ on one or two $Ga$ atom sites are small and therefore, the chemisorption reactions control the growth. The growth rate as a function of growth time was observed to be oscillatory and the growth front was $As$-stabilized. In the case of CLRI growth, the rates of dissociating chemisorption reactions are high and therefore do not control the growth. But, the availability of a proper surface $Ga$ configuration for the efficient incorporation of $As_2$ depends on the surface migration rate of $Ga$. Growth rate as a function of time was constant without oscillation and the growth front was less $As$-stabilized.

Vvedensky et. al. [13] proposed a growth model to study the kinetics of MBE for monitoring surface growth in combination with MC simulations by calculating the evolution of the surface step density. Their model is one, with a single species, in which monatomic deposition avoids the incorporation effects. The model includes adsorption and migration processes. Evaporation is neglected, since for typical temperatures at which the growth is carried out there is negligible dissociation flux from the surface and incorporation probability is assumed to be unity. As in the solid-on-solid (SOS) the growing substrate is modelled by a two dimensional matrix, the entries are the heights of columns of atoms at that point. Their model differs from the SOS model only in that evaporation is neglected.

The evolution of the step density is shown to have a remarkable correspondence to that of the measured RHEED specular spot intensities for III-V semiconductor compounds. Vvedensky et. al. studied growth in a variety of systems, as a function of substrate temperature and drew conclusions concerning the relation between RHEED measurements, kinetics, and growth quality.

Venkatasubramanian [14] developed a stochastic rate equation model based on the master equation approach, QCA and the SOS restriction to simulate the MBE growth of compound semiconductors. His model is based on the SK model. Firstly, the molecular beams used for growing the crystal consist only of monatomic atoms. Secondly, the atoms adsorb only at sites satisfying modified solid on solid (MSOS) restriction. In other words, if the atoms arrive at sites where only one covalent bond can be formed, then the atoms desorb back into vapor. Thirdly, the interlayer diffusion of atoms is allowed to take place between any two layers in the sublattice.

Even though the SK model is generalized to crystals with any in-plane coordination number, it is applicable to one-sublattice crystal only. But, the stochastic model by Venkatasubramanian is suitable for zinc blende crystals and also for compound semiconductor alloy.

Venkatasubramanian [15] used the stochastic model to study the MBE growth kinetics of a hypothetical compound semiconductor and diamond cubic alloy. He employed the model to study the effects of high temperatures due to high surface diffusion rate on the growth rate, the surface roughness, and the clustering phenomenon. One of the important features of the stochastic model is that it is not limited by the crystal size and can be employed to study the doping kintics in the crystals. Its major limitation is that it does not keep track of the surface atomic configuration. It can be obtained from the available data using random distribution approximation.

Computer modeling of $GaAs$ growth has resulted in a better understanding of the kinetics of the MBE growth of $GaAs$. These studies have proved that computer modeling is a viable and complimentary tool for understanding the growth kinetics of MBE. The limitation of these studies are: 1) all of them employ a rigid lattice gas model of size about $30 \times 30 \times 30$ or so and therefore are not suitable for studies on stoichiometries and doping; 2) because of the size limitation, the conclusions are qualitative and at best semi-quantitative; 3) even though MC simulation of kinetics of MBE growth can be employed as a complimentary tool to experiments, it requires extensive experimental data such as surface migration parameters, desorption parameters and the incorporation parameters to be of value to develop the growth kinetic model; 4) the kinetic model employed was specified to $GaAs$ MBE growth and therefore, needs to be generalized to study other material systems.

# Chapter 3

# Surface Kinetic Processes in the MBE Growth of GaAs (100)

In this chapter, the stochastic model of MBE growth is employed to study the surface roughening kinetics in $GaAs$ (100). Firstly, a brief discussion of the stochastic model of MBE growth is presented. Then the results of the study of surface roughening kinetics of (100) $GaAs$ are presented and compared with the experimental work of Ref.[6]. Based on the results, a physical mechanism which adequately describes experimental observation is presented. Finally, a summary of this study is presented.

## 3.1 The Stochastic Model

The stochastic model is a rate equation model based on the condition of detailed balance. It describes the time evolution of semiconductor epilayer through a detailed description of macrovariables in terms of rates of surface processes. The surface processes considered in the stochastic model are: adsorption, evaporation, and migration. Two types of surface migration processes, intralayer and interlayer migrations are considered. The main assumptions of the model are: (i) solid-on-solid (SOS) restriction (ii) random distribution approximation of the surface atomic configurations weighted by the energy of the configuration (iii)Arrhenius type rate equations for the surface kinetic processes (iv) exclusion of anti-site defects (v) exclusion of effects of surface reconstruction on the surface kinetic processes. The primary macrovariables are the concentration of the atoms in the $n^{th}$ layer, C(n), and the atom vacancy bond density in the $n^{th}$ layer, Q(n), as given by Eqs. 8a and 8b of Ref.[14]. These processes are pictorially represented in Fig. (3.1).

The rate of of adsorption can be written as the product of surface sites satisfying the modified solid on solid, MSOS, restriction and the flux rate. The MSOS, employed in this model implies that two nearest neighbor surface atoms be present before an atom gets incorporated at a site in between them at a layer just above as shown in Fig. (3.2). Only the evaporation of atoms exposed to vapor is considered since these atoms have the lowest binding energy and hence a higher probability of evaporation. The rate of evaporation is determined as a product of the fraction of a layer exposed to the vapor, the rate of evaporation of an isolated atom, and the term involving the binding energy of the atom.

The atoms that arrive at non-MSOS sites are allowed to migrate rapidly in their physisorbed state until they find a proper site, either within the layer (intra migration) or in the other layers (inter migration). Unlike in the MC studies in which the interlayer diffusion is allowed only between adjacent layers in the same sublattice, the stochastic model allows interlayer diffusion of atoms between any two layers in the same sublattice.

The evaporation and surface migration processes are described by Arrhenius type rate equations such as:

$$R = R_o \, e^{-\frac{E_{act} + nK_{aa}}{kT}} \tag{3.1}$$

where R is the rate in events/sec. and $R_o$ is the frequency factor of the process in sec$^{-1}$. $E_{act}$ is the activation energy of the process for an isolated terrace adatom, $K_{aa}$ is the second nearest neighbor pair interaction energy in the (100) plane and $n$ is the number of in-plane nearest neighbors of the atom under consideration. Thus, the activation energy term appearing in the argument of the exponential is coverage dependent with $n$ equal to zero and four for low and high coverages, respectively. In general, the $E_{act}$ for surface migration is smaller than that of evaporation. In this study, the $E_{act}$ for interlayer and intralayer migrations are assumed to be equal. The surface migration of an atom to non-MSOS site is not allowed.

### 3.1.1 Macrovariables

Zinc blende crystals have two sublattices, cation and anion sublattices. Therefore, two sets of macro-variables, one for each sublattice, should be defined. In the case of $GaAs$, the cation ($Ga$) is assumed to belong to the even sublattice and the anion ($As$) to the odd sublattice. The macrovariables that can be defined for the $2n^{th}$ layer are: concentration variable, $C_{Ga}(2n)$, the second nearest neighbor atom – vacancy bond density, $Q_{Ga}(2n)$, the second nearest neighbor atom – atom bond density, $\tilde{N}_{GaGa}(2n)$. These above described varibles involve only one layer. In other words, the bonds used in the description of the above variables are inplane bonds.

$$\tilde{N}_{GaGa}(2n) = 2\, C_{Ga}(2n) - \frac{1}{2} Q_{Ga}(2n)$$

for $Ga - Ga$ bond density,

and

$$\tilde{N}_{vv}(2n) = 2\, C_V(2n) - \frac{1}{2}Q(2n) \tag{3.2}$$

for vacancy-vacancy bond density.

The vacancy density, $C_V(2n)$ in the above equation is given by:

$$C_v(2n) = (1.0 - C(2n)),$$

and

$$C(2n) = C_{Ga}(2n)$$

and

$$Q(2n) = Q_{Ga}(2n) \tag{3.3}$$

similar equations can be written for the anion sublattice (i.e.), $As$. In the derivation of equations (3.2) and (3.3), the inplane coordination number is assumed to be four.

In this study, $Ga$ is present in the cation sublattice and $As$ in the anion sublattice. Thus, two independent macrovariables for cation sublattice and two independent macrovariables for the anion sublattice should be considered to study the kinetics of MBE growth of $GaAs$. The independent variables considered are: $C_{Ga}(2n)$, $Q_{Ga}(2n)$, $C_{As}(2n+1)$ and $Q_{As}(2n+1)$.

The rate equation of $Ga$, one of the two sublattices in the diamond cubic crystal ($GaAs$) is given below :

$$\frac{dC_a(2n)}{dt} = \frac{1}{\tau_{ra}} \left( \left[ \frac{\tilde{N}_{bb}(2n-1)}{2} - C_a(2n) \right] e^{L_a} \right. \tag{A}$$

$$- \left[C_a(2n) - 2C_b(2n+1) + \frac{\tilde{N}_{bb}(2n+1)}{2}\right] \left[\frac{\tilde{N}_{aa}(2n)e^{-2k_{aa}} + \frac{1}{2}Q_a(2n)}{2C_a(2n)}\right]^4 \Bigg) \qquad (B)$$

$$+ \frac{4}{\tau_d^{intera}} \left( \left[\frac{\tilde{N}_{bb}(2n-1)}{2} - C_a(2n)\right] e^{L_{oa}} \right. \qquad (C)$$

$$- e^{L_{pa}} \left[C_a(2n) - 2C_b(2n+1) + \frac{\tilde{N}_{bb}(2n+1)}{2}\right] \left[\frac{\tilde{N}_{aa}(2n)e^{-2k_{aa}} + \frac{1}{2}Q_a(2n)}{2C_a(2n)}\right]^4 \Bigg) \qquad (D)$$

where, term A of the above equation corresponds to the adsorption process, term B corresponds to the evaporation process, term C corresponds to the intermigration of atoms to the $n^{th}$ layer from other layers and term D corresponds to the interlayer migration of atoms to other layers from the $n^{th}$ layer.

Similarly, equations for the time evolutions of the macrovariables $Q_{Ga}(2n)$, $C_{As}(2n+1)$ and $Q_{As}(2n+1)$ can be written. For the details of the model, the reader is directed to Ref.[14,15].

### 3.1.2 Boundary Conditions

The boundary conditions for the growth of the compound semiconductor $GaAs$ is discussed in this section. It is assumed that the substrate is flat and that it consists of four layers- the first two layers of the cation ($Ga$) and the other two, anion ($As$) sublattices. The initial conditions for the independent macrovariables are given by:

$$\begin{aligned} C_{Ga}(2n) &= 1.0 \qquad n = 1,2 \\ &= 0.0 \qquad n = 3, ...., \infty \end{aligned}$$

$$\begin{aligned} C_{As}(2n-1) &= 1.0 \qquad n = 1,2 \\ &= 0.0 \qquad n = 3, ..., \infty \end{aligned} \qquad (3.4)$$

$$Q_{Ga}(2n) \quad = \quad 0.0 \qquad n \; = \; 1, \ldots\ldots, \infty$$

and

$$Q_{As}(2n+1) \quad = \quad 0.0 \qquad n \; = \; 1, \ldots\ldots, \infty \tag{3.5}$$

## 3.2 The *GaAs* system : the model and output parameters

The model parameters for the present study of the MBE growth of *GaAs* were obtained from the literature and the MBE growth parameters of Ref.[6].

The material parameters such as $Ga - Ga$ and $As - As$, second nearest neighbor pair interaction energies are obtained from the data reported in Ref.[26].

$$V_{Ga-Ga} = 0.25 \text{ eV}$$

$$V_{As-As} = 0.325 \text{ eV}$$

The frequency factors for the evaporation and migration processes were chosen as 1.0 x $10^{13}$/sec. The activation energy for surface migration of isolated $Ga$ and $As$ atoms was chosen as 1.3 eV based on Ref.[8]. Based on Ref.[8], the activation energy for evaporation of an isolated $As$ was chosen as 1.675 eV.

The MBE growth parameters for this study were obtained from the experimental data given in Ref.[6]. The growth temperature was chosen in the range 723 – 873°K and the flux rate was set at 2 Å/sec. The cation to anion flux ratio employed for the study was in the range 1 : 10 to 1 : 20. It is noted that the (100) substrate surface employed in this study is flat without any steps.

RHEED (reflection high energy electron diffraction) is a technique to study the growth kinetics and chemistry which occur on the substrate surface, using a specular beam of electrons. In this technique, an electron beam is made incident on the growing crystal surface and the intensity of the reflected electron beam (e-beam) from the crystal surface is measured. The intensity of the reflected e-beam depends on the type of interference (constructive or destructive) pattern undergone by the reflected electrons. Also, the interference pattern depends upon the path traversed, which in turn depends upon the roughness of the surface. If the growing surface is smooth, the reflected electrons show constructive interference pattern giving rise to a strong RHEED intensity.

In this study, the intensity of a specular spot ($1^o$ off Bragg) of reflection high energy electron diffraction system with 10 kV electron beam was calculated using kinematical theory of electron diffraction as a function of growth time.

$$TRI(T) = \int_0^t I(t,T)dt \qquad (3.6)$$

where I(T) is the instantaneous RHEED intensity of Off-Bragg specular spot based on kinematical theory of electron diffraction.

The time averaged RHEED intensities, $TRI$(T), were calculated for various growth temperatures.

The material and growth data discussed above were employed to calculate the model parameters according to the procedure detailed in section IVB of Ref.[14]. The model parameters were obtained as a function of growth temperature. The time evolution equations given by Eqs 8a and 8b with modifications discussed in Eq 4, and the boundary conditions corresponding a flat substrate described by Eq 14 of Ref.[14] were solved numerically on a CRAY YMP 2/216 at NSCEE, UNLV, Nevada. The CPU time for a typical growth of 20

Å of $GaAs$ was about 4 hours.

## 3.3 Results and discussions

Concentration profiles were obtained as a function of time for various growth temperatures. They are shown for 823°K, 848°K and 873°K in Fig. 3.3a-c, respectively, for flux ratio 1 : 10. Below 823°K, the concentration profiles look similar to the profile of 823°K and therefore are not displayed. From Fig. (3.3), it is observed that at and below 823°K, the growing surface is $As$-stabilized as is expected when the cation to anion flux ratio is 1 : 10. As the temperature increases, the growth surface becomes less $As$-stabilized. It is also observed that the time delay between the growth of the $Ga$ and subsequent $As$ layers is constant throughout the growth of the $As$ layer for temperatures below 823°K. Above 823°K, the time delay is larger at the start of growth of $As$ layer compared to the the completion of the layer. The decrease in the time delay within the growth of a monolayer of $As$ is almost linear with time. This effect is prominent and larger for higher temperatures and lower flux ratios.

The above observations about the time evolution of the concentration profiles can be explained as follows. The growth of an $As$ layer is controlled by two surface processes; adsorption and evaporation. At temperatures lower than 823°K, the evaporation of surface $As$ is negligible. Therefore, the growth rate is equal to the adsorption rate, which is constant during the growth of a layer. Thus, the time delay during the growth of the layer is constant with time. If the temperature is above 823°K, the temperature is high enough that the evaporation of surface $As$ begins. The growth of an $As$ layer is now controlled by the competition between the adsorption and evaporation processes. The growth rate is the difference between the adsorption rate and evaporation rate. The adsorption rate is independent of the coverage, whereas, the evaporation rate critically depends on the coverage through the activation energy for evaporation which is the binding energy of the atom as discussed under Eq. (3.1). The binding energy of a surface $As$ pair increases with coverage. Therefore, at the start of the growth of an $As$ layer, the binding energy of the $As$ pair is the smallest possible and therefore, the evaporation rate is the largest as given by Eq. (3.1). The growth rate given by the difference between the constant adsorption rate and the large evaporation rate is small. Therefore, there is a large time delay at the start of the growth. As the coverage increases, (i.e., $n$ increases), the $As$ atoms attain more nearest neighbors, and hence their binding energy increases which results in a decrease of the evaporation rate as given by Eq. (3.1). Then, the growth rate increases with the coverage, which results in a continuous decrease of the the time delay. The time delay is more at higher temperature, due to an increase in the evaporation rate and at lower flux ratio due to smaller adsorption rate. The concentration profiles under similar temperature conditions but for a cation to anion ratio of 1:20 are shown in Fig. 3.4a-c. The observed time delay for this flux ratio is found to be less than that for flux ratio 1:10. This is because, at higher flux ratio (1:20) the rate of adsorption of $As_2$ is twice faster and hence the coverage increases at faster rate. Thus intraplanar nearest neighbors, n, increases twice the rate of flux ratio 1:10 resulting in the decrease of time delay. Thus, at lower temperatures and higher flux ratios, the surface appears more $As$-stabilized. The description of the surface processes is in complete agreement with the mechanisms proposed in Ref.[6] based on the experimental observations.

The intensity of a specular spot ($1^\circ$ off Bragg) of reflection high energy electron diffraction system with 10 kV electron beam was calculated using kinematical theory of electron diffraction as a function of growth time. The time averaged RHEED intensities, $TRI$(T), were calculated for various growth temperatures. A plot of $TRI$(T) versus growth temperature is shown in Fig. (3.5) for flux ratios 1 : 10 and 1 : 20. The $TRI$(T) decreases below and above a certain value of T called the transition temperature, and is identified as 770°K and 800°K, respectively, for flux ratios 1 : 10 and 1 : 20. The lower $TRI$(T) above and below the transition temperature is directly related to rougher surface. Below the transition temperature, the thermal activation for surface migration is low and therefore, the $Ga$ and $As$ atoms randomly adsorb on the surface at sites of their arrival resulting in a rough surface. As temperature increases towards the transition temperature, the thermal activation and hence surface migration increases resulting in adatoms finding energetically more stable sites. This surface process decreases the surface roughness. Above the transition temperature, the evaporation of $As$ begins resulting in a rougher surface. The roughness of the surface directly correlates with decreased RHEED intensity due to destructive interference of the electron waves reflecting from various surface layers. Thus, the RHEED intensity peaks at the transition temperature. The flux ratio dependence of $TRI$(T) can be explained as follows. Lower flux ratio results in longer time for the formation of surface atom clusters with more than two $As$ atoms. This implies that the average evaporation rate during the growth of monolayer of $As$ is larger due lower coverage dependent activation energy for evaporation and hence lower transition temperature. This is in good agreement with the work of Chen et. al. [6].

The plot of $TRI$ versus temperature obtained in this study was compared with that of the experimental study of Chen et al. [6] and semi-quantitative agreement between the results was obtained. There are two main reasons for the quantitative differences between the results: (i) The molecular species is employed for the experiments ($As_4$) and our work ($As_2$) are different. (ii) the flux ratios employed in the experiment and our work may be different as experimental flux ratios are always reported in equivalent beam pressure ratios not in terms of rates of arrival of anion to cation as done in our work. Both of these can influence the result of transition temperature quantitatively.

## 3.4 Summary

The stochastic model of MBE growth based on the master equation approach with solid-on-solid restriction and quasi-chemical approximation is employed for the study of surface processes in (100) $GaAs$ growth. The growth rate, the time averaged surface roughness and the time averaged RHEED intensity were obtained for various growth temperatures. The kinetic surface roughening transition temperature for the MBE growth of $GaAs$ is identified as 770°K and 800°K for flux ratios 1 : 10 and 1 : 20, respectively, from the temperature dependence of the time averaged RHEED intensity. The results of this study compare favorably with that of the experiments obtained under similar growth conditions[6]. The phenomenon of kinetic surface roughening transition in the MBE growth of GaAs (100) is explained in terms of the competition among various surface processes such as the incorporation and evaporation of atoms which roughen the surface and the surface migration of atoms to energetically favorable sites which smoothens the process.

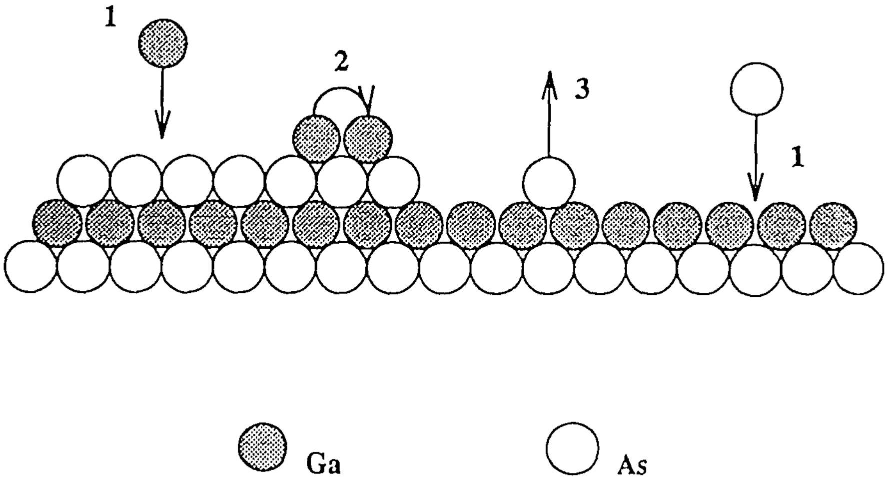

Figure 3.1: A schematic representation of atomistic picture of all the kinetic processes that are considered for the simulation: (1) incorporation, (2) surface migration, (3) reevaporation.

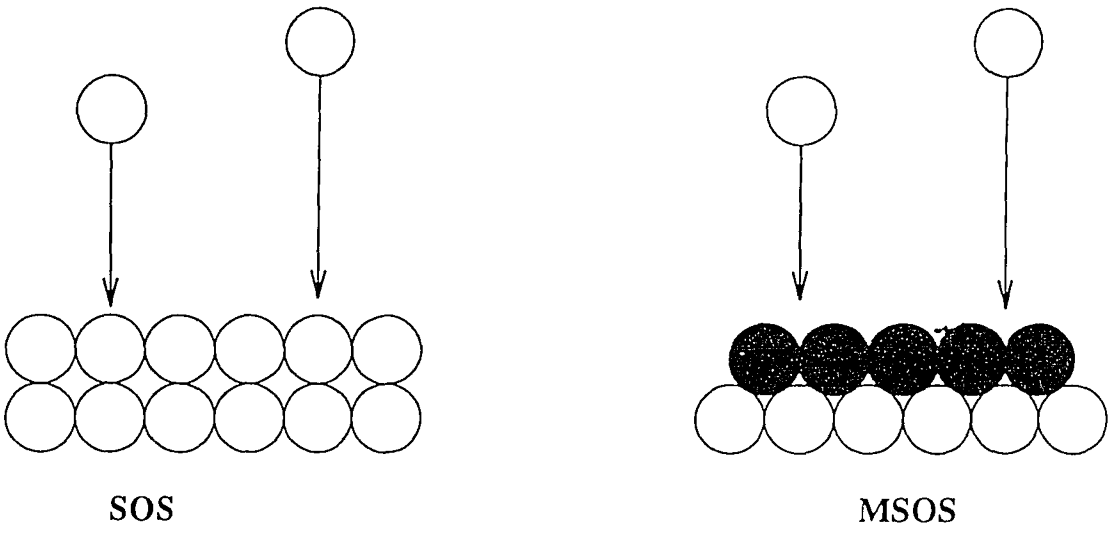

Figure 3.2: A pictorial representation of the MSOS restrictions.

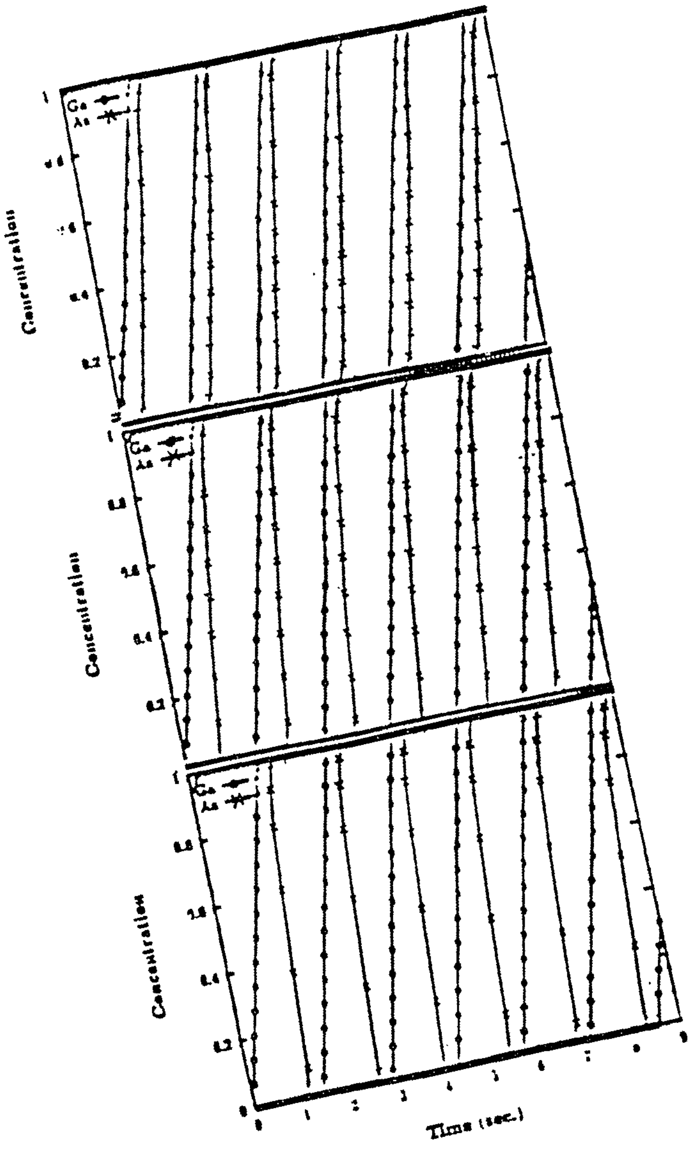

Figure 3.3: Concentration profiles of $Ga$ and $As$ for flux ratio 1:10 for various temperatures. (a) 823K (b) 848K (c) 873K.

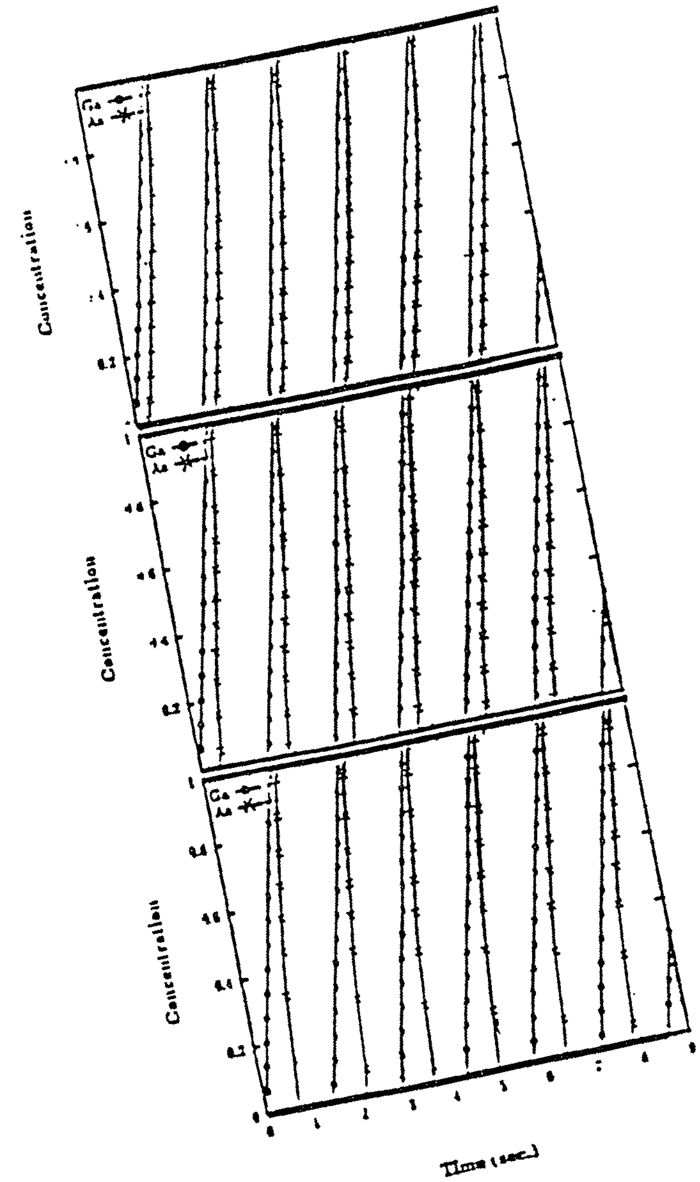

Figure 3.4: Concentration profiles of $Ga$ and $As$ for flux ratio 1:20 for various temperatures. (a) 823K (b) 848K (c) 873K.

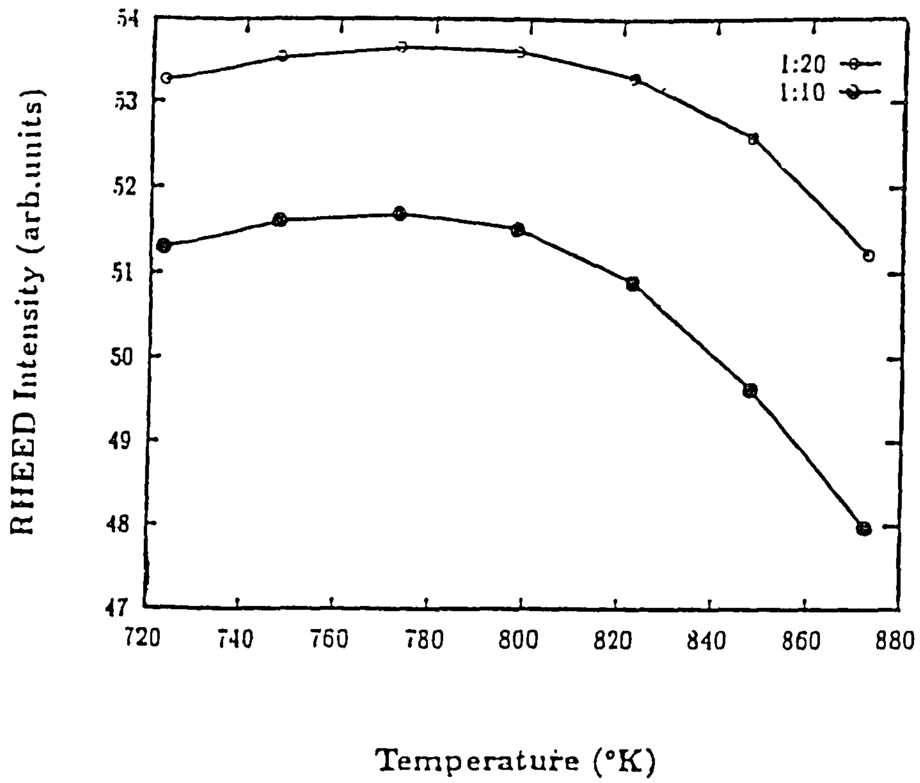

Figure 3.5: Time averaged RHEED intensity versus temperature for flux ratios (a) 1:10 (b) 1:20.

# Chapter 4

# MBE Doping Kinetics

In this chapter, a rate equation model based on the master equation approach is developed for the study of MBE doping kinetics. The model includes elementary surface processes such as adsorption, evaporation and migration of atoms. First, the model is used to study the surface segregation phenomenon during $In$ doping of $Si$. Then the time and growth rate of the dopant segregation phenomenon are studied. The model is used to study $\delta$ doping of dopants. Finally, a summary of this study is presented.

## 4.1 Rate Equation Model for Doping

The elementary surface kinetic processes that control the doping kinetics are: adsorption, evaporation and interlayer migration of the the host atom, $Si$, and the dopant, $In$, ($In$ is chosen for this study, but the model is general and can be applied to any system). The rate of change of concentration of $Si$ in the $n^{th}$ layer can be written in terms of the rates of the microscopic kinetic processes discussed above. Describing the time evolution of the concentration of $Si$ in the $n^{th}$ layer, $C(n)$, we obtain:

$$\begin{aligned}
\frac{dC_{Si}(n)}{dt} = {} & J_{Si}\,[C(n-1)-C(n)] && (A)\\
& - R_o e^{\frac{-E_{ave,eva,Si}}{kT}}\,[C(n)-C(n+1)]\left(\frac{C_{Si}(n)}{C(n)}\right) && (B)\\
& + R_o e^{\frac{-E_{ave,dif,Si}}{kT}}\,[C(n-1)-C(n)]\left(\frac{C_{Si}(n+1)}{C(n+1)}[C(n+1)-C(n+2)]+\frac{C_{Si}(n-1)}{C(n-1)}[C(n-1)-C(n)]\right) && (C)\\
& - R_o e^{\frac{-E_{ave,dif,Si}}{kT}}\,[C(n)-C(n+1)]\left(\frac{C_{Si}(n)}{C(n)}\right)([C(n+1)-C(n+2)]+[C(n-1)-C(n)]) && (D)
\end{aligned}$$

$$(4.1)$$

Term $A$ describes the rate of adsorption of $Si$ on to the $n^{th}$ layer in terms of the available sites for adsorption, $[C(n-1)-C(n)]$, and the flux rate, $J_{Si}$. The description in Term $A$ assumes that the atoms adsorb with unity sticking probability at sites which are available for adsorption. Term $B$ describes the rate of loss of $Si$ from the $n^{th}$ layer due to evaporation in terms of the number of atoms exposed to vapor, $\frac{C_{Si}(n)}{C(n)}[C(n)-C(n+1)]$, the frequency factor which is assumed to be $10^{13}$/sec. and the average activation energy for evaporation of $Si$ atoms, which depends on the concentration of the layer. In this description, it is assumed that number of nearest neighbors for a $Si$ atom increases directly as the concentration of $Si$ in the layer. Note that since the dopants are in *ppm* levels, they do not affect the binding energy of $Si$ atoms. Thus, the average activation energy for evaporation of a $Si$ atom in the $n^{th}$ layer, $E_{ave,eva,Si}$, is given by:

$$E_{ave,eva,Si} = E_{iso,eva,Si} + zE_{SiSi}C_{Si}(n) + zE_{SiD}C_D(n) \qquad (4.2)$$

where $z$ is the inplane coordination number which is 4 for (001) plane and 6 for (111) plane. $E_{SiSi}$ and $E_{SiD}$ are the second nearest neighbor interaction energies of $Si-Si$ and $Si-D$

pairs, respectively and $E_{iso,eva,Si}$ is the activation energy for evaporation of an isolated $Si$ atom on the surface. Here $D$ denotes dopant. (Note that within the (001) and (111) planes, the nearest neighbor atoms are actually the second nearest neighbor atoms when the whole crystal is considered.) Term $C$ in Eq. (4.1) is the rate of gain of $Si$ atoms in the $n^{th}$ layer due to interlayer migration of $Si$ to the $n^{th}$ layer from the adjacent layers, $n-1$ and $n+1$. Term $D$ in Eq. (4.1) is the rate of loss of $Si$ atoms in the $n^{th}$ layer due to interlayer migration of $Si$ from the $n^{th}$ layer to the adjacent layers, $n-1$ and $n+1$. The average activation energy for the migration of $Si$, $E_{ave,dif,Si}$ is given by:

$$E_{ave,dif,Si} = E_{iso,dif,Si} + zE_{SiSi}C_{Si}(n) + zE_{SiD}C_D(n) \tag{4.3}$$

where $E_{iso,dif,Si}$ is the activation energy for interlayer migration of an isolated $Si$ atom.

A similar equation for the rate of change of dopant concentration in the $n^{th}$ layer can be written by simply replacing $Si$ with $D$. In the rate equation for the dopant, the activation energy for evaporation and migration should be redefined as:

$$E_{ave,eva,D} = E_{iso,eva,D} + zE_{SiD}C_{Si}(n) + zE_{DD}C_D(n) \tag{4.4}$$

and

$$E_{ave,dif,D} = E_{iso,dif,D} + zE_{SiD}C_{Si}(n) + zE_{DD}C_D(n) \tag{4.5}$$

respectively, where $E_{DD}$ is the $D-D$ atom pair interaction energy.

## 4.2 Results and Discussion

Two cases, $In$ doping of $Si$ and $B$ delta doping of $Si$, are studied using the model proposed in section 4.1.

### 4.2.1 In doping of Si

In the description of Equations (4.4) and (4.5), the fact that the second nearest neighbors of dopant atoms are essentially $Si$ atoms due to the $ppm$ level concentrations of $In$ has been utilized. The activation energy for the evaporation of an isolated $Si$, $E_{iso,eva,Si}$, has been predicted for (100) and (111) growths to be 2.6 eV and 3.2 eV, respectively [27]. The second nearest neighbor interaction energy, $E_{SiSi}$ for (100) and (111) growths are estimated to be 0.25 eV and 0.325 eV, respectively [27]. The activation energy for evaporation of $In$ is not reported in the literature. Thus, a trial and error approach was taken to fit two of the data points on the concentration of $In$ versus $\frac{1}{T}$ plot reported in Ref.[28]. We obtained a value of 1.6 eV and -0.25 eV for $E_{iso,eva,In}$ and $E_{SiIn}$, respectively. The activation energy for migration of an isolated $Si$, $E_{iso,dif,Si}$, was chosen as 0.8 eV based on available experimental data for activation energy for $Si$ [26]. $E_{iso,dif,In}$, was assumed to be equal to that of $Si$ for lack of available data.

The growth parameters were chosen exactly as used for the experimental work reported in Ref.[29] and are presented below. The flux rate of $Si$, $J_{Si}$, was kept at $1\mu$m/hr. The flux ratio between $Si$ and $In$, $J_{In}/J_{Si}$, was maintained at $2 \times 10^{-4}$. The evaporation of $Si$ was negligible in the temperature range of this study and therefore the growth rate of the epilayer was approximately equal to the $J_{Si}$. The substrate temperature was in the range $500 - 750^{\circ}$C.

The differential equations given by Eq. (4.1) and a similar one for $In$ are coupled nonlinear first order differential equations which are not analytically integrable. Therefore, these equations were solved numerically on a CRAY YMP2. The boundary condition is that the first 4 layers are full with $Si$ and rest of the layers are empty at the start of the growth which corresponds to assuming an atomically flat substrate. A typical run for a growth of 20 seconds took about 1 CRAY CPU hour.

Plots of the $In$ sticking coefficient, $S_{In}$, versus time (sec.) for various growth temperatures of the study were obtained and analyzed. (The growths were simulated only for about 20 seconds due to computer time limitations.) Analysis of the data indicated that $S_{In}$ is an exponentially decaying function of time. Exponentials of the form $A(T)e^{-\frac{t}{\tau(T)}}$ were fitted for each temperature. Note that $A(T)$ and $\tau(T)$ are functions of temperature. Using $A(T)$ and $\tau(T)$, $S_{In}$ was obtained for the case of 3000 seconds of growth by extrapolation. Such an extrapolation is justified because the growth rate is constant and the layer-by-layer growth mode is maintained for all growth conditions in this study.

A plot of the extrapolated $S_{In}$ versus $\frac{1}{T}$ is shown in Fig. (4.1) along with the experimental data. The agreement between the theoretical values and the experimental values from Ref.[29] is excellent for the entire temperature range. The mechanism which results in the temperature dependence of $S_{In}$ is as follows. At low temperatures, the surface segregation aided evaporation of $In$ (due to its repulsive interaction with the host sublattice) is not dominant as the thermal energy is not enough to allow this activated process. As temperature increases, the interlayer migration rate of $In$ to the surface increases and the $In$ concentration increases in the surface layer. More $In$ in the top surface layer, results in more opportunities for evaporation. Thus, a larger evaporation of $In$ results at higher temperature. The evaporation rate of $In$ aided by the surface segregation process is much larger than the typical evaporation rate of atoms from the surface.

Plots of the dopant concentration, $C_{In}$, versus distance from the surface are shown in Fig. (4.2) for various growth times at 660°C. It is observed that the $In$ concentration in the bulk is about the same and is independent of the time of growth. The surface concentration of $In$, however, is increasing with time as expected. Note that there is a dip in $C_{In}$ for all the profiles just below the surface layer. The concentration of $In$ in this zone is an order of magnitude less than that in the bulk and many orders of magnitude less than that at the surface. We call this region the dopant depleted zone (DDZ). The physical reason for this phenomenon is as follows. The dopant, $In$, segregates from the layers below upwards due to the repulsive atomic interaction with the host lattice. In other words, considering the $n^{th}$ layer, $In$ atoms migrate from the $n - 1^{th}$ layer to the $n^{th}$ layer which increases $C_{In}(n)$ and to the $n + 1^{th}$ layer from the $n^{th}$ layer which decreases $C_{In}(n)$. The rates of these processes depend on the availability of $In$ atoms in the respective layers that are exposed to vapor so that they can migrate and the availability of sites in the respective layers. For the migrations to the $n^{th}$ layer compared to the migrations from the $n^{th}$, both of these factors are small. Thus, the rate of migration to the surface layer from the subsurface layer is larger than rate of migration of $In$ to the subsurface layer from one layer below. This difference in the rates results in a deficiency of $In$ atoms in the subsurface layer. This resembles the phenomenon of a precipitation depleted zone (PDZ) which occurs near the grain boundaries in many alloys. This result was compared with the experimental data and a careful observation of the segregation profile data shown in Fig. (2) of Ref.[29] does show that there is a dip in the profile. In our result the dip is much more pronounced compared to that of the experiments, which may be due to stronger repulsive interaction energies used in our model.

Plots of the $In$ segregation profiles for 853°K, 893°K, and 933°K are shown in Fig. (4.3). It appears that the segregation profiles are similar for various temperatures except that the bulk $In$ concentrations are lower for higher temperature which correlates well with Fig. (4.1). This type of a dopant depleted zone may not always be present even if the dopant interactions with the host lattice is repulsive. It depends on a variety of factors such as the growth rate, the strength of the repulsive interaction ($E_{SiIn}$), the flux ratio, $J_{Si}/J_{In}$ and others.

### Growth Rate and Time Dependence

The growth at 933°K was studied as a function of growth rate in the range 0.2 to 2 monolayers/sec with the dopant flux at 2 x $10^{-4}$ monolayers/sec. A plot of dopant concentration versus growth rate is shown in Fig. (4.4). The sticking coefficient decreases with growth rate due to increased evaporation. As a layer nears completion, the activation energy for $In$ evaporation decreases increasing its evaporation rate ($In$ is squeezed out of the layer). If more layers are grown without increasing the dopant flux, the increased evaporation rate will yield a smaller sticking coefficient.

The surface concentration of $In$ during $Si$ growth at 933°K was studied as a function of growth time. A plot of the surface concentration of $In$ versus growth time is shown in Fig. (4.5). This observation agrees quantitatively with the results of Ref.[24] where a functional dependence of the form $1 - exp(\frac{-t}{\tau})$ was obtained.

### 4.2.2 Delta Doping of Si

Unlike the previous study, here dopants are deposited in a layer in large concentration. Therefore, dopant-dopant pair interactions cannot be neglected and Eqs. 4.2-4.5 were used without any simplifications.

$\delta$-doping of $Si$ with $B$ and $Sb$ have been successfully attempted to achieve more precise control of the doping profile (of the order of tens of Å) and a very high dopant concentration (as high as $10^{21}/cm^3$) in the MBE growth of $Si$ [25,30]. Because the energy parameters for the $Si - B$ and $Si - Sb$ systems are unknown, a hypothetical dopant, $D$, is used in the $\delta$ doping studies of $Si$. Even though one of the model parameters is chosen arbitrarily, the mechanisms illustrated and the knowledge gained through this study are valid for many real systems.

The growth parameters chosen for the $\delta$ doping study were taken from Ref.[30] based on $B$ doping of $Si$. The shutter sequence for $\delta$ doping is as follows. $Si$ was grown at 2 $\mathring{A}$/sec. for 2 seconds and then the $Si$ shutter was closed and simultaneously the $In$ shutter was opened. Then, 0.3 monolayer of $In$ was deposited within 1 second. Then the $In$ shutter was closed and simultaneously the $Si$ shutter was opened. The $Si$ growth was continued for 17 seconds after closing the dopant shutter. The total layer thickness of $Si$ grown was about 40 $\mathring{A}$. The growth temperatures for the study were in the temperature range 673°K to 973°K. Many studies were carried out for $D - D$ pair interaction energies in the range of -$E_{SiD}$ to $E_{SiD}$. The influence of $E_{DD}$ was found to be negligible, the results presented here corresponds to $E_{DD}$ = 0.0 eV. Two sets of calculations with the interaction energies between $Si$ and dopant ($E_{SiD}$), -0.08 eV (strong repulsion) and -0.01 eV (weak repulsion) were made and are reported.

The panels in Fig. 4.6a and b show plots of $In$ concentration as a function of the depth of the layers for two cases (i.e.), -0.08 eV and -0.01 eV, respectively. For case 1 Fig. 4.6a, it is noted that the peak of the dopant concentration has shifted more towards the surface at high temperatures compared to low temperatures. In other words, the dopant profile has shifted away from the layers where they were intended to be. This observation can be explained as follows. High temperatures result in strong surface segregation of $D$ due to increased surface migration. At low temperature the surface migration and hence the surface segregation are minimal and therefore, the bulk of $D$ atoms incorporate very close to or at the intended layers. Due to small repulsive interaction used in Fig. (4.6b), such a shift in the peak of $D$ concentration is not observed.

The other interesting and possibly counter-intuitive observation in Figures 4.6a and b is that as the temperature increases, the breadth of the dopant profile decreases. In other words, higher temperatures result in sharper dopant profiles. This observation is in good qualitative agreement with the results of the experimental work on the $\delta$ doping of $Si$ with $B$ [30]. Even though, the authors of Ref.[30] have attributed this to possible higher error in experimental data due to rounded profiles, our work suggests a possible physical explanation which is as follows. First, let us observe that the area under the curves of Figures 4.6a and b for all temperatures are about equal indicating negligible evaporation in this temperature range. The sharpness of the dopant profile at higher temperature is due to the atomically smooth surface on which the dopants are incorporated. At low temperatures the growth surface is somewhat rougher and the segregation effect is smaller and therefore, the $D$ atoms incorporate at lower unfilled layers and segregate to upper filled layers, resulting in a broader dopant profile.

The model presented in this article is general and can be applied to any MBE doping system with any growth orientation. The model under special conditions may yield analytical solutions which will be helpful for process automation. Results of the present study show that doping kinetics is intimately linked to growth kinetics of the semiconductor epilayer. Many of the theoretical models assume that the semiconductor growth kientics is decoupled from the dopant kinetics which is correct only under limited circumstances. The limitations of the model is that it requires parameters such as pair interaction energies and activation energies. This limitation is not unique to our model, but is typical of any theoretical study of kinetics. The other limitation of the model is its inability to grow thick epilayers on the order of several microns in a reasonable amount of computer time. In this study, this limitation is overcome by extrapolation of the results. It should be noted that such extrapolation schemes may not always be applicable.

## 4.3 Summary

A rate equation model based on the master equation approach is developed for the study of MBE doping kinetics. The model is applied to study the surface segregation phenomenon observed during $In$ doping of $Si$. The doping studies were performed for various growth conditions. The predicted sticking coefficient of $In$ versus $\frac{1}{T}$ and the dopant depth profile shows excellent agreement with experiments. The dopant sticking coefficient decreases with $T$ due to surface segregation aided evaporation of $In$ at higher temperatures. The surface segregation of $In$ occurs due to strong repulsive interaction between $In$ and the host lattice which results in upward migration of $In$. A dopant depleted zone where the $In$ concentration is lower than that in the bulk and at the surface is observed and agrees well with experiments. The time and growth rate dependences of the phenomenon are studied and found to agree with work reported in the literature. $\delta$ doping of $Si$ is studied in the range of $673^{o}k$ to $973^{o}K$. The results are in qualitative agreement with experimental results. With an increase in temperature, the dopant profiles become sharper which is explained by smoother growth surface at higher temperatures.

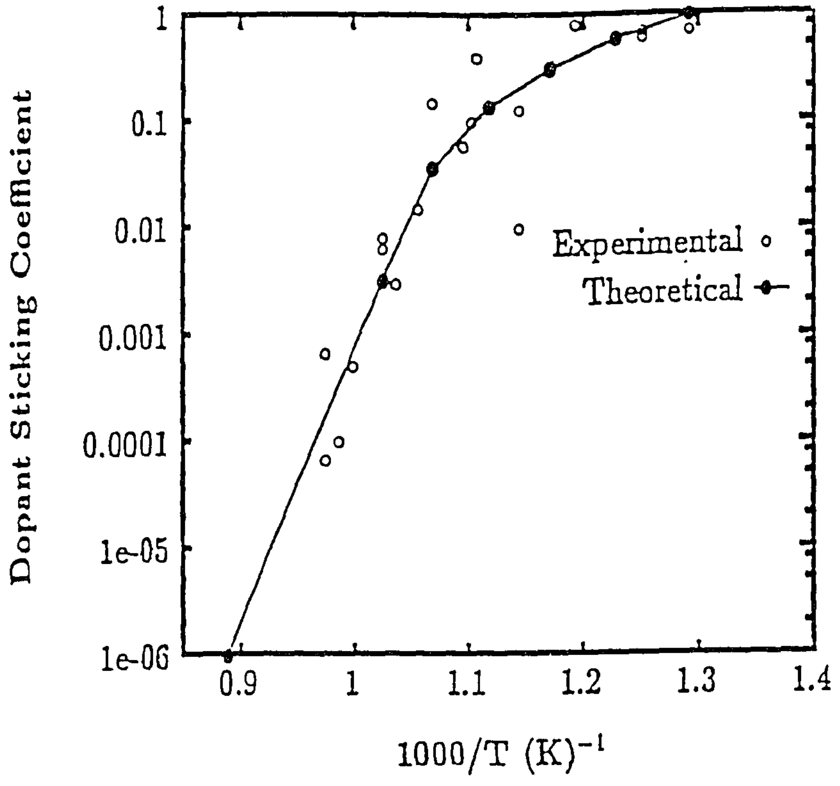

Figure 4.1: Sticking coefficient of the dopant, $In$, versus $\frac{1}{T}$.

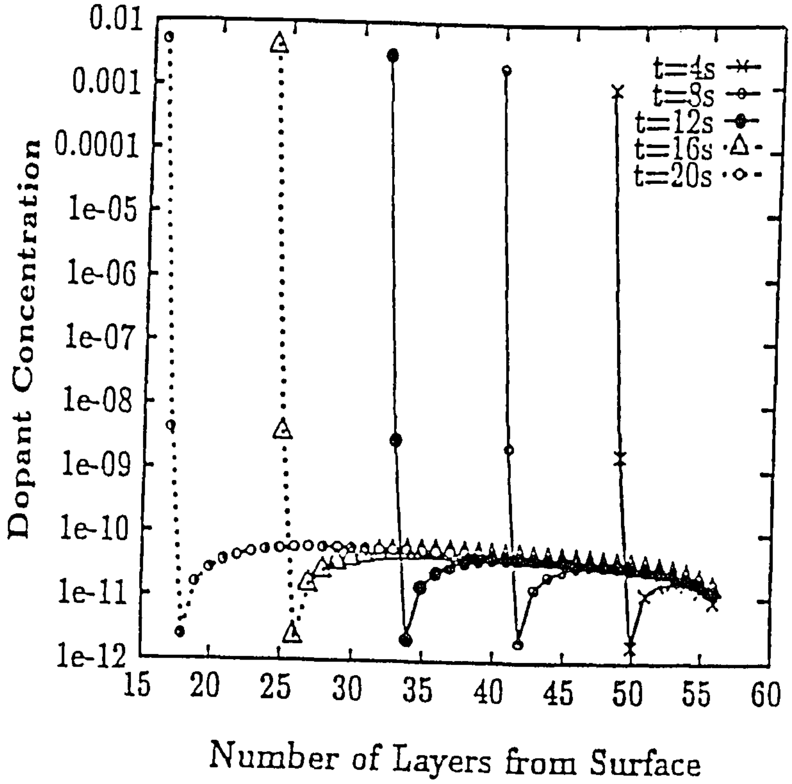

Figure 4.2: Dopant segregation profile for various growth times for growth at 933°K.

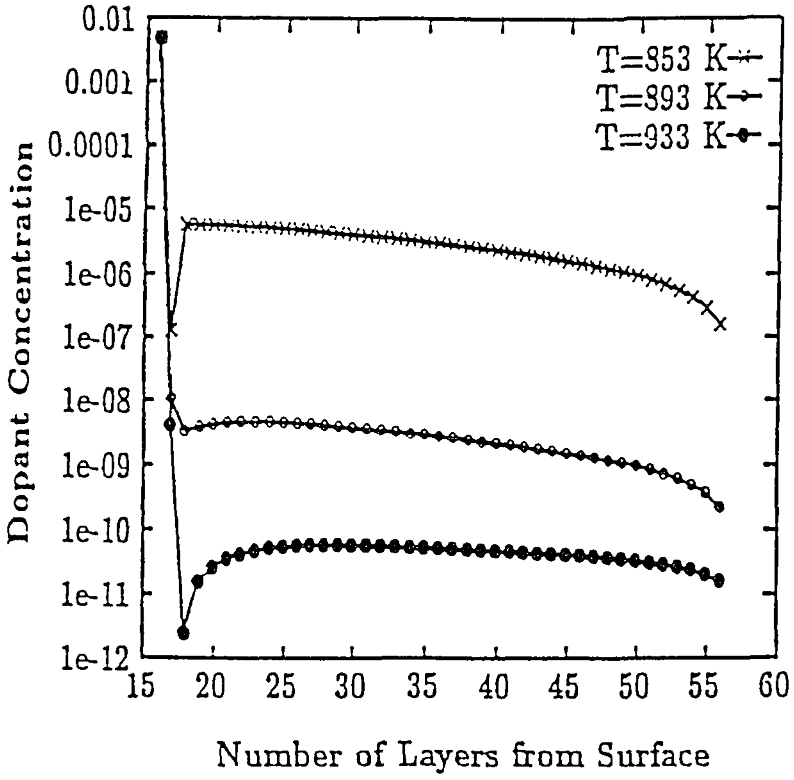

Figure 4.3: Dopant segregation profiles for various temperatures for a growth time of 20 seconds.

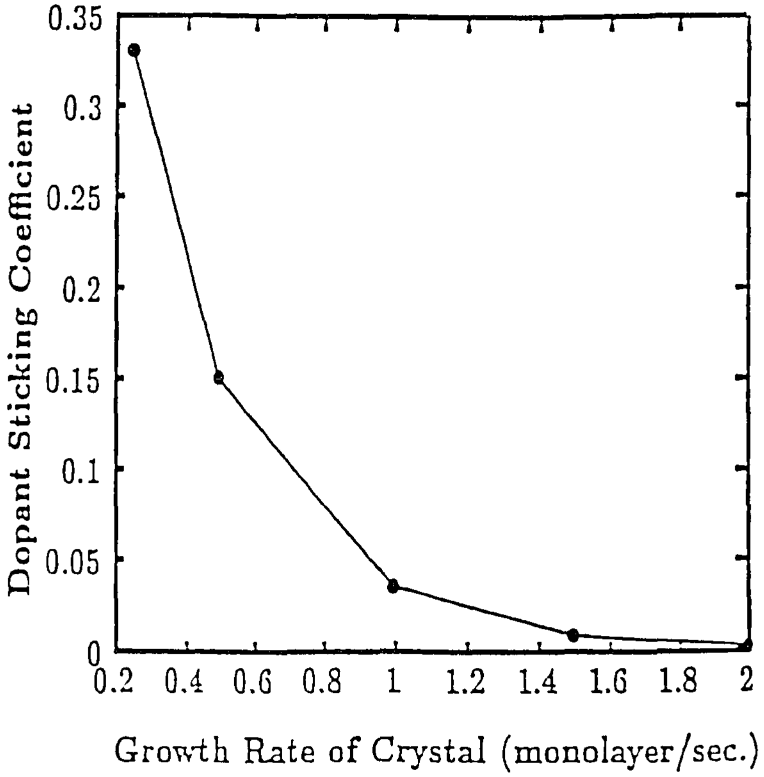

Figure 4.4: Dopant sticking coefficient for various growth rates at 933°K.

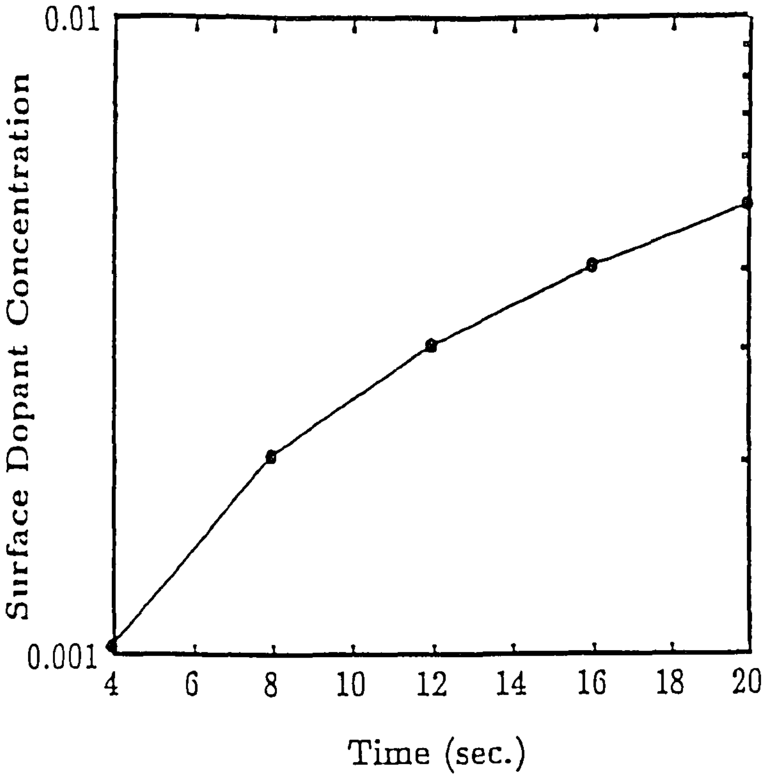

Figure 4.5: Surface concentration of dopant for various growth times at 933°K.

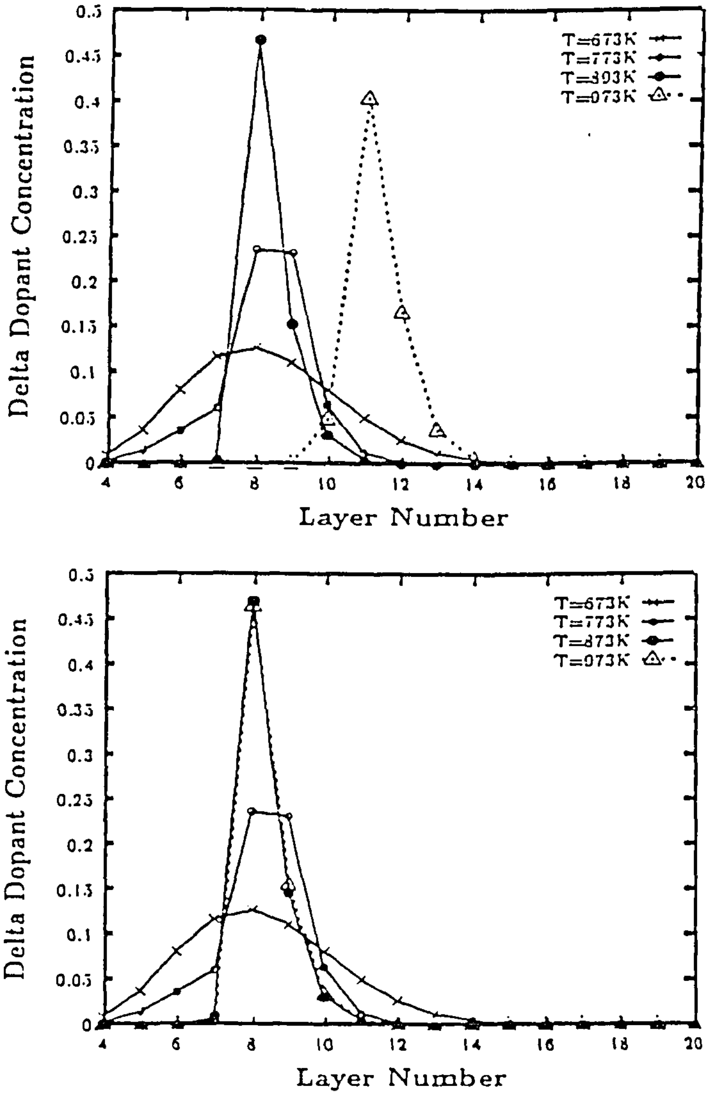

Figure 4.6: Delta doping profiles with (a) $E_{SID}$ = -0.08 eV (strong repulsion) and (b) $E_{SID}$ = -0.01 eV (weak repulsion) at 933°K.

# Chapter 5

# Conclusion

The surface kinetics of MBE growth of (100) $GaAs$ and doping kinetics of $In$ doped $Si$ system were studied theoretically using a stochastic model based on the master equation approach with the solid-on-solid restriction and a quasi-chemical aproximation for various growth conditions. The growth rate, the time averaged surface roughness and the time averaged RHEED intensity were obtained for various growth temperatures. The kinetic surface roughening transition temperature for the MBE growth of $GaAs$ is identified as 770°K and 800°K for flux ratios 1 : 10 and 1 : 20, respectively, from the temperature dependence of the time averaged RHEED intensity. The results of this study compare favorably with that of the experiments obtained under similar growth conditions[6]. The phenomenon of kinetic surface roughening transition in the MBE growth of GaAs (100) is explained in terms of the competition among various surface processes such as the incorporation and evaporation of atoms which roughen the surface and the surface migration of atoms to energetically favorable sites which smoothens the process. In the study of surface segregation phenomenon of dopants, the predicted sticking coefficient of $In$ versus $\frac{1}{T}$ and the dopant depth profile shows excellent agreement with experiments. The dopant sticking coefficient decreases with $T$ due to surface segregation aided evaporation of $In$ at higher temperatures. The surface segregation of $In$ occurs due to strong repulsive interaction between $In$ and the host lattice which results in upward migration of $In$. A dopant depleted zone where the $In$ concentration is lower than that in the bulk and at the surface is observed and agrees well with experiments. The time and growth rate dependences of the phenomenon are studied and found to agree with work reported in the literature. $\delta$ doping of $Si$ is studied in the range of $673^o$ K to $973^o$ K. The results are in qualitative agreement with experimental results. With an increase in temperature, the dopant profiles become sharper which is explained by smoother growth surface at higher temperatures.

Based on the present work, and as a continuation of this work, the following studies are recommended. (1)Develop the stochastic model to study other growth observations such as (111). (2)Use the present model to study other material systems. (3)Explore ways to relax the SOS restriction. (4)Develop a model to obtain microstructural information from the output of the stochastic model.

# Bibliography

[1] Tsao J.Y., "Fundamentals of Molecular Beam Epitaxy," *Academic Press Inc., 1993.*

[2] Einspruch N.G., Cohen S.S., Singh R.N., "VLSI Electronics Microstructure Science, Beam Processing Technologies, vol.21," *Academic Press Inc., 1989.*

[3] Foxon C.T. and Joyce B.A., "Interaction kinetics of $As_4$ and $ga$ On 100) $GaAs$ surfaces using a modulated molecular beam technique", *Surface Sci.*, vol. 50, (1975), p434.

[4] Foxon C.T. and Joyce B.A., "Interaction kinetics of $As_2$ and $Ga$ on 100 $GaAs$ surfaces", *Surface Sci.*, vol. 64, (1977), p293.

[5] Foxon C.T., "MBE growth of $GaAs$ and III-V alloys", *J. Vac. Sci. Tech.*, vol B 1, (1983), p293.

[6] Chen P., Kim J.Y. and Madhukar A., "Optimal surface and growth front of III-V semiconductors in molecular beam epitaxy: A study of kinetic processes via RHEED specular beam intensity measurement on $GaAs$ (100):, *J. Vac. Sci. Tech.*, vol B 4, (1986), p890.

[7] Saito Y. and Krumbhaar H.M., "Diffusion and relaxation kinetics in stochastic models for crystal growth", *J. Chem. Phys.*, vol. 70, (1979), p1078.

[8] Arthur J.R., "Surface stoichiometry and structure of $GaAs$", *Surface Sci.Surface Sci.*, vol. 43, (1974), p449.

[9] Weeks J.D., Gilmer G.H., and Jackson K.A., "Analytical theory of crystal growth", *J. Chem. Phys.*, vol. 65, (1976), p712.

[10] Weeks J.D., Gilmer G.H., and Jackson K.A., "SOS model for defect-free simple cubic [100] crystal growth", *Adv. Chem. Phys.*, vol. 40, (1979), p157.

[11] Madhukar A. and Ghaisas S.V., "Study of RHEED oscillation behaviour as a function of arsenic pressure for low substrate temperatures", *Appl. Phys. Lett.*, vol 47, (1985), p3.

[12] Singh J., Bajaj K.K., "Theoretical studies of the intrinsic quality of $GaAa/AlGaAs$ interfaces grown by MBE: Role of kinetic processes", *J. Vac. Sci. Tech.*, vol. B 3, (1985), p520.

[13] CLARK S. AND VVEDENSKY D.D., "Growth kinetics and step density in RHEED during molecular-beam epitaxy", *J. Appl. Phys.*, vol. 63, (1988), p2272.

[14] VENKATASUBRAMANIAN R., "MBE growth of compound semiconductors: Stochastic modeling", *J. Matl. Res.*, vol. 7, (1992), p1222.

[15] VENKATASUBRAMANIAN R., "MBE growth of compound semiconductors: Applications of Stochastic modeling", *J. Matl. Res.*, vol. 7, (1992), p1236.

[16] IYER S.S., METZGER R.A., AND ALLEN F.G., "Sharp profiles with high and low doping levels in $Si$ grown by molecular-beam epitaxy", *J. Appl. Phys.*, vol. 52, (1981), p5608.

[17] WOOD C.E.C., DESIMONE D., SINGER K., AND WICKS G.W., "Magnesium-and calcium doping behaviour in molecular-beam epitaxial III-V compounds", *J. Appl. Phys.*, vol. 53, (1982), p4230.

[18] BEAN J.C., "Arbitrary doping profiles produced by $Sb$-doped $Si$ MBE", *Appl. Phys. Lett.*, vol. 33, (1978), p654.

[19] OTA Y., "$n - type$ doping technique in $Si$ molecular-beam epitaxy by simultaneous arsenic ion implantation and antimony evaporation", *J. Electrochem. Soc.*, vol 126, (1979), p1761.

[20] BECKER G.E. AND BEAN J.C., "Acceptor dopants in silicon molecular-beam epitaxy", *J. Appl. Phys.*, vol 48, (1977), p3395.

[21] ROCKETT A., BARNETT S.A., GREENE J.E., KNALL J., AND SUNDGREN J.E., "Dopant depth distribution as a function of growth temperature in $In$-doped (100) $Si$ grown by molecular-beam epitaxy", *J. Vac. Sci. Tech.*, vol. A 3, (1985), p855.

[22] STREIT D., METZGER R.A., AND ALLEN F.G., "Doping of $Si$ in molecular-beam epitaxy systems by solid phase epitaxy", *Appl. Phys. Lett.*, vol 44, (1984), p234.

[23] BARNETT S.A. AND GREENE J.E., "$Si$ molecular beam epitaxy: A model for temperature dependent incorporation probabilities and depth distributions of dopants exhibiting strong surface segregation", *Surface Sci.*, vol. 151, (1985), p67.

[24] ANDRIEU S., AVITAYA F.A., AND PFISTER J.C., "Surface segregation mechanism during two-dimensional epitaxial growth: The case of dopants in $Si$ and $GaAs$ molecular-beam epitaxy", *J. Appl. Phys.*, vol 65, (1989), p2681.

[25] PARRY C.P., KUBIAK R.A., NEWSTEAD S.M., WHALL T.E. AND PARKER E.H.C., "Temperature dependence of incorporation processes during heavy boron doping in $Si$ molecular beam epitaxy", *J. Appl. Phys.*, vol 71, (1992), p118.

[26] NEAVE J.H., DOBSON P.J., AND JOYCE B.A., "RHEED oscillations from vicinal surfaces-a new approach to surface diffusion measurements", *Appl. Phys. Lett.*, vol 47, (1985), p100.

[27] KRISHNAMURTHY S., BERDING M.A., SHER A., AND CHEN A.B., "Energetics of molecular-beam epitaxy models", *J. Appl. Phys.*, vol. 68, (1990), p4020.

[28] KNALL J., SUNDGREN J.E., GREENE J.E., ROCKETT A., AND BARNETT S.A., "Indium incorporation during the growth of (100) *Si* by molecular beam epitaxy: Surface segregation and reconstruction", *Appl. Phys. Lett.*, vol 45, (1984), p689.

[29] TABE M. AND KAJIYAMA K., "Study of doping kinetics in *In* doped *Si* system", *Jpn. J. Appl. Phys.*, vol 22, (1983), p423.

[30] JORKE H., AND KIBBEL H., "Boron delta doping in *Si* and $Si_{0.8}Ge_{0.2}$ layers", *Appl. Phys. Lett.*, vol. 57, (1990), p1763.

[31] GREENE J.E., BARNETT S.A., ROCKETT A., AND BAJOR G.J., "Modelling of dopant incorporation, segregation, and ion/surface interaction effects during semiconductor film growth by molecular beam epitaxy and plasma-based techniques", *Appl. Surface. Sci.*, vol. 22/23, (1985), p520.

[32] CHASON E., TSAO J.Y., HORN K.M., AND PICRAUX S.T., "Dynamics of growth roughening and smoothening on *Ge* (100)", *J. Vac. Sci. Tech.*, vol B 7, (1989), p332.

[33] MORKOC H, DRUMMOND T.J., AND FISHER R., "Interfacial properties of (*Al*, *Ga*) *As*/*GaAs* structures: Effect of substrate temperature during growth by molecular beam epitaxy", *J. Appl. Phys.*, vol 53, (1982), p1030.